

# Behavior of the electron spin resonance signals in X-ray irradiated human fingernails for the establishment of a dose reconstruction procedure

Seiko Hirota\*, Chryzel Angelica B. Gonzales and Hiroshi Yasuda

Department of Radiation Biophysics, Research Institute for Radiation Biology and Medicine (RIRBM), Hiroshima University, Kasumi 1-2-3, Minami-ku, Hiroshima City, Hiroshima 734-8551, Japan

\*Corresponding author. Department of Radiation Biophysics, Research Institute for Radiation Biology and Medicine (RIRBM), Hiroshima University, Kasumi 1-2-3, Minami-ku, Hiroshima City, Hiroshima 734-8551, Japan. Email: [hirota-seiko@hiroshima-u.ac.jp](mailto:hirota-seiko@hiroshima-u.ac.jp)  
(Received 20 September 2020; revised 2 February 2021; editorial decision 26 February 2021)

## ABSTRACT

The retrospective dosimetry that follows accidental X-ray exposure is becoming more significant for improving radiation diagnosis and treatment. We investigated the dosimetric properties of electron spin resonance (ESR) signals in X-ray irradiated fingernails under conditions that resemble realistic situations. We collected fingernails from 12 Japanese donors between the ages of 30 to 70. The sampled fingernails were utilized for X-ray irradiation, mechanical stimulation and background measurements. We also collected 10 toenails from one of the donors to evaluate their differences from fingernails. Additionally, we prepared 15 samples from two donors to compare the signals generated by  $\gamma$ -rays to those by X-rays. After observing the linear dose–response for both X- and  $\gamma$ -ray irradiated samples, we found that the sensitivity of the air-absorbed dose of  $\gamma$ -ray irradiated samples was identical to that of X-ray irradiated samples. The effect from secondary electrons seemed to be small in fingernails. The inter-individual variation in the sensitivity was no greater than the intra-individual variation. The signal intensities in each measurement fluctuated about the linear response curve, and the size of the fluctuation was dependent on the sample. The average fluctuation corresponded to 1.7 Gy, and the standard deviation was 1.3 Gy. The signal induced by X-rays could be erased by soaking the samples in water and subsequently drying them for four days, which allowed us to estimate the signal intensity prior to the exposure. These characteristics of the ESR signal induced by X-rays facilitate the development of a feasible protocol for fingernail dose reconstruction.

**Keywords:** electron spin resonance (ESR); electron paramagnetic resonance (EPR); fingernail; toenail; retrospective dosimetry

## INTRODUCTION

The investigation of electron spin resonance electron paramagnetic resonance (EPR) signals from human fingernails after a radiation accident can be useful for retrospective dosimetry [1]. In most studies [2], researchers have used  $\gamma$ -ray sources such as Cesium-137 or Cobalt-60, which have been the common sources of radiation exposure in past accidents. Accordingly, published reports have established the minimum detectable dose [3], fading patterns of ESR signals [1, 4] and an appropriate sample preparation process [5, 6] for  $\gamma$ -rays. Based on these studies, Trompier *et al.* [5, 6] were the first to report the use of fingernails for ESR dosimetry after  $\gamma$ -ray radiation accidents.

One of the most significant issues related to the establishment of fingernail ESR dosimetry is the difficulty of separating the

radiation-induced signal (RIS) from the mechanically-induced signal (MIS) and the background signal (BKS). The RIS was discovered in 1989 [1], when suitable materials to use for retrospective dosimetry were being sought. The investigator confirmed that the signal growth depends on the given radiation dose and they noticed that the RIS spectrum was similar to the MIS spectrum. The MIS was known at this time, because the ESR signal from non-irradiated human nails generated by cutting had already been discussed in 1987 [7] in an investigation of the ESR signals from sulfur-centered radicals [8]. The existence of the BKS was also noticed in the studies conducted during this period [9]. Investigators found this residual component after the eliminating the rest of signal. They speculated that the BKS might be caused by ambient radiation, which generates radicals in the

equilibrium state [9]. Both the MIS and the BKS overlap with the RIS; the RIS appears in the regions where the  $g$ -factor is 2.005. In each signal, several components with different  $g$ -factors exist, which indicates that various radicals are generated inside human nails by stimuli such as radiation and mechanical cutting [10]. At the resolution of the X-band ESR, the ESR peaks from these various radicals are convolved and the broad singlet spectrum appears at room temperature. To separate these three types of signals and their corresponding components, characteristics such as the  $g$ -factor, the microwave power dependence and stability have been investigated [10, 11]. Moreover, in the past 20 years, a number of studies have sought to identify the origin of each type of radical [4, 7, 9, 12, 13].

However, these studies only qualitatively investigated the MIS and BKS and researchers tried to remove them by physical and chemical means. There was no attempt to determine the effect from these noise sources and conduct an analytical removal. These studies also suggested protocols for use during sample collection, storage and measurement, but they are too complicated for nail ESR to be widely useful for retrospective dosimetry in actual radiation accidents. Thus, we need to study the behavior of these signals under realistic conditions and subsequently propose a new procedure based on practical experience and evaluate its limitations.

The previous studies also lacked much needed information, especially when the focus of the research is on X-ray irradiation. While X-rays are the most commonly used technique for diagnosis and treatment (e.g. for computed tomography [CT], fluoroscopy, etc.), the detailed characteristics of the ESR signals induced by X-rays are still unclear. For example, no reports have yet been published about the basic dosimetric properties of different types of radiation. Thus, it is necessary to determine the dose–responses characteristics of the fingernail ESR signals in order to effectively utilize them in the analysis of accidental exposures.

X-ray sensitivity is the most important property that needs to be determined. Therefore, we initially measured the X-ray sensitivity of fingernails and studied the factors that affect it. We focused primarily on the type of radiation and on inter- and intra-individual variations. To our knowledge, this was the first systematic investigation of these characteristics that was conducted without any build-up materials, such as real accidents. We expect this information to be useful for optimizing the calibration curve in the case of an actual radiation accident.

In addition, to estimate the RIS from an exposure accident, we need to know not only the sensitivity of the fingernails, but also the BKS and MIS at harvest. In general, the initial state of each sample prior to the exposure and the actual signal generated at harvest by mechanical means are unknown. We can only measure the convolution of the BKS and MIS at harvest with the accident-induced RIS. To reconstruct the accident-induced RIS, we need to subtract both the BKS and MIS at harvest from the ESR signal measured after the harvest of the exposed samples. Thus, we need to establish the method for evaluating the MIS and BKS of each sample. One study [2] reported an increase in the MIS component under ambient conditions; this results from the plastic deformation of the  $\alpha$ -keratin helix [14], which is a primary component of fingernails. Methods to erase the MIS without affecting the RIS were introduced by treating the samples with water [2, 10, 11] or chemicals [16]. However, in a more realistic situation, the samples resulting from an accident will be sent by mail; hence, we need to devise

a method to estimate the MIS component in the samples at the time of measurement. We report our efforts to accomplish this in the present article. In particular, we quantitatively evaluate the sensitivity induced by mechanical cutting as there are no detailed quantitative reports at present. We also report our estimation of the BKS signal. In addition, we measure the BKS after eliminating both the RIS and MIS at harvest by soaking the samples in water [16] and compare it to the BKS estimate using the method described in this study. Based on these results, we recommend a protocol for utilizing X-ray irradiated nails for retrospective dosimetry. We also measure the distribution of non-irradiated samples, for which we expect the signal to be simply the convolution of the MIS and BKS. As far as we know, there has been no previous report regarding this, especially with respect to Japanese donors. In addition, if the strength of the BKS and MIS display inter-individual variation, we would need to compare samples within the same donor. We therefore measure the characteristics of toenails as well in order to judge whether they can be compared to the sampled fingernails.

The structure of this article is as follows. In RIS SENSITIVITY FOR X-RAYS, we report the measurements of the RIS sensitivity of fingernails to X-rays, from methods to results and discussion. The methods for and results of estimating the MIS and BKS are addressed in DETERMINATION OF THE MIS AND BKS. We tried estimation based on the MIS sensitivity and direct measurement of the BKS in termination from MIS response and direct measurement of BK, and we also tried to estimate integrated MIS and BKS by direct measurements from non-irradiated samples after cutting them in Determination from non-irradiated samples are cutting. Based on the results and known findings, we proposed new procedures for utilizing nail ESR dosimetry in X-ray exposure accidents in section PROPOSAL OF NEW PROCEDURE FOR NAIL ESR DOSIMETRY. Lastly, we summarize and conclude our study in section 5.

### RIS SENSITIVITY FOR X-RAYS

We examined the dose–response of fingernail samples for X-rays up to a maximum of 93.6 Gy using multiple irradiations (added doses). The following subsection discusses the details of sample preparation and storage, irradiations and ESR measurements. We defined sensitivity as the signal increase per 1 Gy per 1 mg of the sample. We represent the dose as the air-absorbed dose, which we measured using glass dosimeters (see X-ray irradiation).

For comparison, we also performed the dose–response measurements for  $\gamma$ -rays in the same way as for X-rays (see  $\gamma$ -ray irradiation). It is worth mentioning that we did not use phantoms to obtain the secondary electron equilibrium because the fingernails are located on the surface of the body. Instead, we calculated the samples' real absorbed dose by using a Particle and Heavy Ion Transport Code System (PHITS) calculation to estimate the effects of the lack of build-up material and understand the differences in the sensitivity between the two types of radiation.

## Materials and Methods

### Sample preparation and storage

We collected fingernail samples from a total of 12 Japanese donors, who ranged from 30 to 70 years of age. Table 1 shows the characteristics, such as sex, age and finger position, of the X-ray irradiated samples

**Table 1. Sample information, resolution of detection and sensitivity of fingernails in the X-ray irradiation case**

Sample information (Donor, Age, Sex)	Finger Position	Sample Weight [mg]	Fluctuation [Gy]	Sensitivity [1/Gy/mg]
Donor 1 (59, male)	Right Thumb	16.1	1.3	0.0042
	Right Index	14.7	1.0	0.0031
	Right Middle	13.6	2.0	0.0057
	Right Ring	14.7	1.0	0.0043
	Right Little	6.0	0.7	0.0048
	Left Thumb	16.7	1.0	0.0046
	Left Index	11.7	1.5	0.0042
	Left Middle	11.3	1.4	0.0036
	Left Ring	9.3	1.7	0.0049
Donor 2 (49, male)	Left Little	4.8	1.0	0.0044
	Right Thumb	35.1	2.2	0.0044
	Right Index	40.4	5.0	0.0041
	Right Middle	18.2	3.2	0.0042
	Right Ring	16.5	0.88	0.0042
	Right Little	11.3	2.1	0.0043
	Left Thumb	25.3	1.2	0.0044
	Left Index	15.4	1.8	0.0046
	Left Middle	10.7	0.69	0.0046
Donor 3 (34, male)	Left Ring	11.7	0.92	0.0043
	Left Little	8.4	0.52	0.004
	Right Thumb	19.5	1.2	0.0057
	Right Index	14.9	1.6	0.0036
	Right Middle	20	0.44	0.0036
	Right Ring	17.5	1.74	0.0034
	Right Little	10.1	5.0	0.0028
	Left Thumb	20.3	0.74	0.0038
	Left Middle	16.8	0.63	0.0051
Donor 4 (33, male)	Left Ring	13.4	1.2	0.013
	Right Thumb	8.9	2.8	0.004
Donor 5 (35, male)	Right Thumb	1.59	5.2	0.005
Donor 6 (34, female)	Right Thumb	6.71	0.75	0.0048
Donor 7 (44, male)	Right Thumb	5.22	2.5	0.0032
Donor 8 (62, female)	Right Thumb	3.57	5.8	0.0026

obtained from eight donors that were used for the sensitivity study. For comparison, we obtained three additional samples for  $\gamma$ -ray irradiation, which were taken from donor 6. Table 2 shows the characteristics for  $\gamma$ -rays. The same treatment was given to all the samples after the harvest. The samples were stored in a dark box with silica gels under ambient conditions with 20% relative humidity at 20°C room temperature. The weight of each sample was 3–20 mg, depending on the donor and the finger position.

The thickness of each fingernail sample was 0.2–0.8 mm, typically being about 0.5 mm thick. Individual pieces were 7–15 mm long and 1–2 mm wide. One sample set consists of several pieces of nails obtained from one specific finger through a one-time harvest during daily life.

#### X-ray irradiation

We performed the X-ray irradiation of the samples using a commercial device (Cabinet X-ray system model CP-100, Faxitron Bioptics LLC.,

Tucson, USA). The X-ray tube was an MXR-160/21 (COMET.AG, Flamatt, Switzerland) with a tungsten target. The X-rays were delivered from a tube with a 160 kV maximum voltage and 10 mA maximum current. In our study, the tube voltage and current were set to 160 kV and 6.3 mA, respectively. The X-ray tube contained filtration (beryllium, 0.8 mm  $\pm$  0.1 mm), and no additional filter was used. The peak photon energy of photons was around 60 keV, and the dose rate was 1.2 Gy/min.

For each round of irradiation with X-rays, the total air-absorbed dose was measured using seven Dose Ace GD-352 M glass dosimeters (Chiyoda Technol Corporation, Tokyo, Japan). This type of glass dosimeter has a filter to provide a stable energy response for photons under 200 keV. The change in the relative response to photons was kept within 10% in the energy range between 30 keV and 700 keV. From 20 keV to 30 keV, the relative response drops down to 0.75 compared to the response to 700 keV photons [17]. The error in the measurement

**Table 2. Sample information, resolution of detection and sensitivity for the  $\gamma$ -ray irradiation case**

Sample information (Donor, Age, Sex)	Finger Position	Fluctuation (Gy)	Sensitivity [1/Gy/mg]
Donor 1 (59, male)	Finger Right Middle	-	0.0055
	Finger Right Ring	-	0.0048
	Finger Right Little	-	0.0048
	Finger Left Middle	-	0.0046
	Finger Left Ring	-	0.0054
	Finger Left Little	-	0.005
Donor 2 (49, male)	Toe Right Middle	-	0.0044
	Toe Right Ring	-	0.0045
	Toe Right Little	-	0.0023
	Toe Left Middle	-	0.0046
	Toe Left Ring	-	0.0049
	Toe Left Little	-	0.0038
Donor 6 (34, female)	Finger Unknown	8.2	0.00086
	Finger Unknown	5.7	0.0012
	Finger Unknown	2.8	0.0012

corresponds to error propagation of the standard deviation from five measurements with all glass dosimeters.

We placed the samples uncovered at the center of the sample table made of 5.6 mm thick acrylic board equipped in the cabinet X-ray system. One glass dosimeter was typically placed within 1 cm of each sample. The X-ray tube was located 28 cm above the table.

We carried out ESR measurement (see ESR measurement) of all the samples prior to the irradiation in order to determine the initial, non-irradiated state. We irradiated each sample repeatedly, and we measured it at 1-hour intervals after each irradiation. The number of data points taken to produce one dose–response curve ranged from 5 to 19, depending on the total dose, 2.9 Gy, 9.5 Gy, 23 Gy, 52 Gy or 93 Gy.

#### $\gamma$ -ray irradiation

We exposed 15 samples to  $\gamma$ -rays using a Gamma-cell40 Exactor Low Dose-Rate Research Irradiator (Best Theratronics Ltd., Ottawa, Canada). In this irradiator, the sample canister (10 cm high and 31.2 cm in diameter) was located between two Cesium-137 sources. The dose rate was 0.79 Gy/min. The air-absorbed dose was monitored using a Dose Ace GD-302 M (Chiyoda Technol Corporation, Tokyo, Japan) glass dosimeter during each irradiation, just as in the X-ray irradiation. We placed the samples uncovered at the center of the sample canister. We placed a glass dosimeter next to each sample and measured the dose–response curves in the same way as for the X-ray irradiation.

#### ESR measurement

We used a JES-FA100 instrument (JEOL Ltd., Tokyo, Japan) with an X-band microwave generator (9.4 GHz) to measure the ESR signals. Examples of ESR spectra with different modulations are presented in Fig. 1. The signal intensity is defined as the peak-to-peak amplitude of the ESR spectrum after linear baseline correction, and it is normalized using the sample weight. The unit of intensity is either a procedure-defined unit (p.d.u.) or an arbitrary unit (a.u.), which are produced

by the JES-FA100 model using the measurement parameters listed in Table 3.

We used a broader modulation amplitude than in the previous studies in order to increase the sensitivity of signal detection. With a broader modulation amplitude, peaks sometimes become duller than the original shapes determined by the inner structures of the samples. However, in our case, we observed similar peak-to-peak line widths for amplitudes from 0.025 mT to 1 mT (Fig. 1). The sensitivity with a 1 mT modulation width is roughly four times higher than that with a width of 0.25 mT. Comparing the signal intensity from the same samples using 1 mT and 0.25 mT modulation widths, the correlation between them was 0.96 in 20 samples. Additionally, we only focused on the peak-to-peak amplitude to measure the dose received in this study. Accordingly, we concluded that a 1 mT modulation amplitude was better to use due to its higher sensitivity.

We placed each sample into a quartz-glass sample tube and then positioned it in the resonant cavity. Due to the solid-state and non-uniform shapes of the samples, we expected some measurement errors with respect to the signal intensity. Therefore, we rotated the sample tube by 45 degrees along its horizontal axis between measurements to minimize any sample-position-induced errors. We averaged the eight resulting spectra to obtain the value of the signal intensity. The most significant contribution to the remaining measurement error was due to the vertical position of the sample in the resonant cavity. We found that if the sample was shifted by 1 mm from the center position, the signal intensity decreased by 4%. In the present study, we used this value as the size of the error bar for the measured ESR signal intensity.

#### PHITS calculation

We roughly calculated the dose absorbed by the samples using PHITS [18] to understand the effect of the absence of any covering materials on the achievement of a secondary electron equilibrium state.

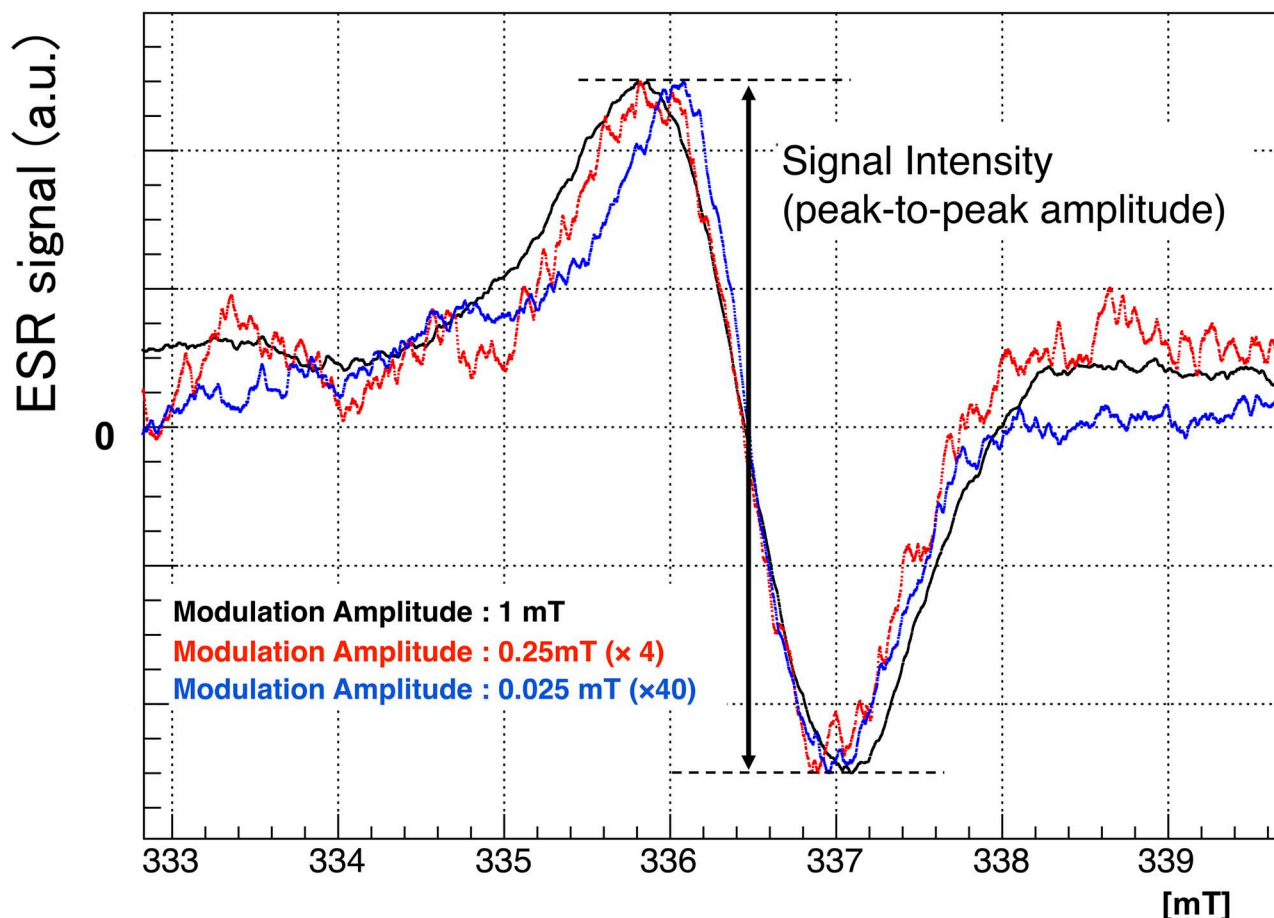


Fig. 1. Typical examples of ESR spectrum from irradiated human nails with different modulation. Amplitude after linear baseline correction. Black, modulation amplitude = 1 mT; red, 0.25 mT; blue, 0.025 mT. Here, the y-axis is normalized by peak-to-peak amplitude to compare the spectrum shape and peak-to-peak width. We defined the signal intensity as the peak-to-peak amplitude with 1 mT modulation amplitude. It increased as given dose increased.

Table 3. Parameters for the ESR measurements in our study

Microwave frequency	9.4 GHz
Microwave power	1 mW
Scanning field	328.5–343.5 mT
Time constant	0.3 sec
Sweep time	30 sec
Modulation amplitude	1 mT
Number of Scan	10 times
Cavity type	cylindrical TE011 cavity

At lower photon energies, photoelectric absorption dominates the process of energy absorption for both X-rays and  $\gamma$ -rays. The cross-section for photoelectric absorption is proportional to the fourth or fifth power of the atomic number and inversely proportional to the

photon energy. The main component of a fingernail is  $\alpha$ -keratin, which includes cysteine—the sulfur-containing amino acid [19]. The atomic number of this element is larger than the value for air and it contributes to a higher energy absorption by fingernails for photon energies of a few tens of keV. For this estimate, we identified the components of the amino acids in fingernails based on a previous study [17 (Table. 1)] that used a sample with a density of 1.0 g/cm<sup>3</sup>. The virtual fingernail sample used for the calculation was 1 cm long, 1 mm wide and 0.5 mm thick. We calculated the dose every 10 keV ranging from 0 keV to 160 keV and 662 keV photons. The cases under 160 keV were for X-ray irradiation, whereas 662 keV was for  $\gamma$ -ray irradiation. The target was placed in a space filled with air, and the photons were generated from 10 cm behind the surface of the target.

## Results and discussion

We observed a linear dose–response in all samples, as shown in Fig. 2 (donor 1, right thumb, X-ray irradiation). The linearity can be seen up to 93.6 Gy, which was the total dose of this sample. The dashed

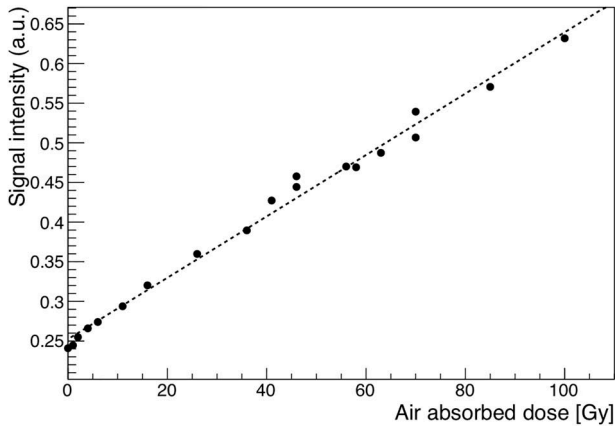


**Fig. 2.** Typical dose–response curve for X-ray irradiation of signal from fingernails. Donor 1, right thumb. In this case, there is linearity in dose–response up to 93.6 Gy. The dotted line shows the best fit of the linear function to the data point.

line shows the best fit of a linear function to the data using the linear regression analysis. The sensitivities are expressed by the slope of the linear functions (i.e. by the signal increase per Gy of air-absorbed dose). The intercept in Fig. 2 is the signal intensity before irradiation, which includes the BKS and the MIS, as well as the increase in the MIS during storage. We will discuss those points later (see Determination from MIS response and direct measurement of BKS and Determination from non-irradiated samples after cutting).

Figure 3 shows the sensitivity distribution for all the samples. The median sensitivity for X-rays was  $(0.0043 \pm 0.0001)/\text{Gy}/\text{mg}$ . For comparison, the median sensitivity for  $\gamma$ -rays was  $(0.0046 \pm 0.0001)/\text{Gy}/\text{mg}$ . The Wilcoxon rank-sum test could not reject the hypothesis that the mother distribution of the sensitivity for  $\gamma$ -rays is the same as for X-rays. Based on these results, we can make a recommendation that you can obtain the calibration curve using  $\gamma$ -ray radiation as for the accidental X-rays exposure under investigation.

To estimate the effects of the lack of build-up materials with respect to the achievement of secondary electron equilibrium and by using the air-absorbed dose as an indicator in our setup, we calculated both the dose distribution and the depth, including secondary-electrons and the ratio of the absorbed X-ray dose of 662 keV (Cesium-137)  $\gamma$ -rays using PHITS. We used the air-absorbed dose in our study, as this is used by X-ray equipment in the medical settings. In general, the actual dose of X-ray and  $\gamma$ -ray irradiation absorbed by the samples differs from the air-absorbed dose.

Figure 4 shows the profile of the absorbed dose with depth in the fingernail substance for the case of the irradiation by 60 keV photons, as calculated by PHITS. The vertical axis is proportional to the absorbed dose, in an arbitrary unit. From this profile, we found the build-up region to be around 0.8 cm for 60 keV photons, which was the most frequently used X-ray energy in our experiment. At the peak position, the absorbed dose is about 6% larger than at the surface. Figures 5a and b show a photon energy scan at the depth of the build-up region and the ratio of the build-up increment in the substance representing nails in the PHITS calculation, respectively. Figure 5a shows

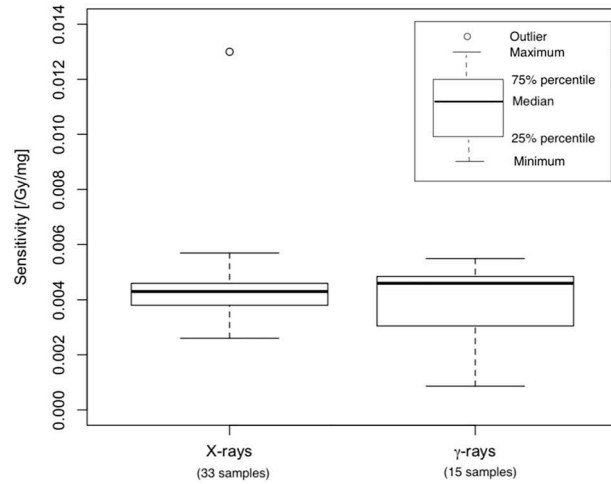


**Fig. 3.** The sensitivity distribution for all samples. The X-ray irradiated samples showed similar sensitivity to  $\gamma$ -ray irradiated samples for the same air absorbed dose.

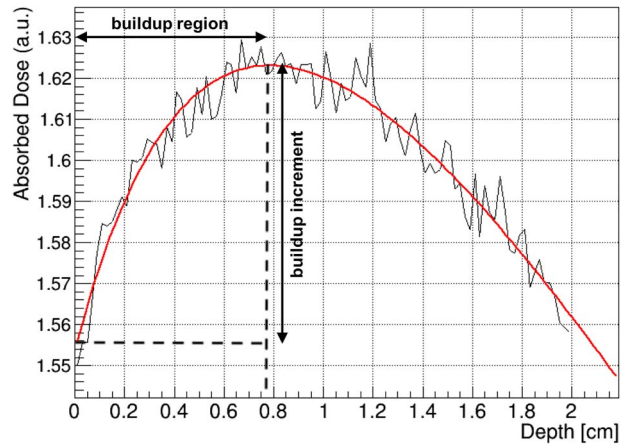


**Fig. 4.** The profile of absorbed dose along to depth of samples by 60 keV photons in PHITS calculation. The vertical axis is proportional to dose but in a.u. The build-up region is 0.8 mm and the absorbed dose increase 6% at the peak.

that the maximum depth of the build-up region was about 0.8 cm, which was achieved with 70 keV photons. In all of the energy regions in our experiment, including both X-rays and  $\gamma$ -rays, our nail samples were totally in the build-up region because their typical thickness was 0.5 mm. However, based on Fig. 5b, the maximum of build-up increment was around 6% in all energy regions. Even for 60 keV photons, for which the build-up is steepest in the first 0.5 mm, the build-up increment was only 0.9%, whereas for 662 keV photons, it was only 0.06%. If we assume that the sample thickness varies from 0.2 mm to 0.8 mm, the change in the absorbed dose ranged from  $-0.8\%$  to  $0.4\%$ . Due to this small ratio of build-up increment for samples around 0.5 mm thick, we concluded that the effects of the lack of build-up material have no significant effects on our research.

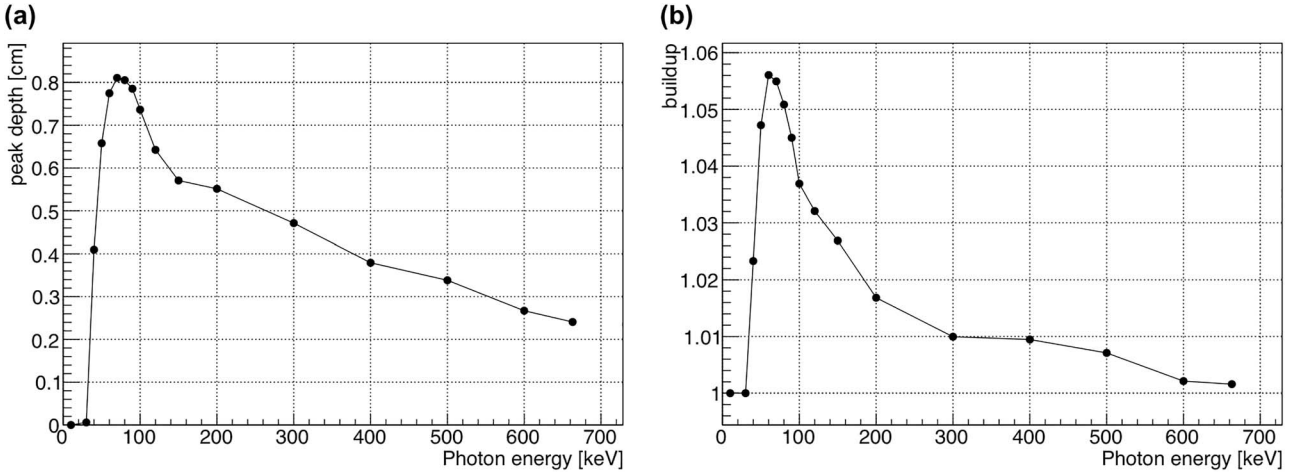


**Fig. 5.** (a) The photon energy dependence of peak depth of build-up in the material assuming nail component in PHITS. The maximum was around 0.8 cm around 70 keV photon energy. (b) The photon energy dependence of build-up increment calculated by PHITS. One refers to the absorbed dose at the surface. The maximum increment was only 5.6% at peak with 60 keV case.

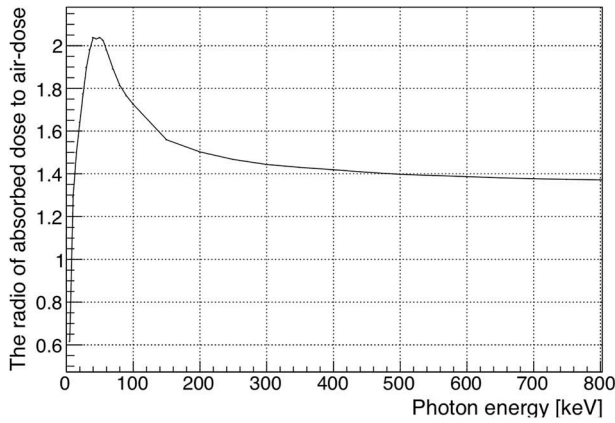


**Fig. 6.** The ratio of absorbed dose in the virtual nail sample (1 cm long, 1 mm wide and 0.5 mm thick) by various energy photons to air-absorbed dose in the same radiation field.

Next, we considered the relationship between the indicated air-absorbed dose and the real dose absorbed in the samples. Figure 6 shows the result of PHITS calculations of the ratio of dose of photons of varying energy absorbed in fingernail samples to the air-absorbed dose in the same radiation field. This figure shows that the maximum ratio is 2.02 at around 50 keV. At 662 keV, which is assumed to be Cesium-137, the ratio is 1.37. Based on these data, we can estimate that the maximum difference of the absorbed dose ratio between X-rays and  $\gamma$ -rays is a factor of 1.47 if the X-ray energy is 50 keV. This is not a bad estimation, because the X-rays we used in our experiment ranged from 10 keV to 160 keV, and the most frequently used energy was 60 keV. Based on this result, if there were no other differences between the two types of radiation except for the absorbed dose, the sensitivity difference for the air dose should be within a factor of 1.5.

Figure 7 shows the sensitivities to X-ray irradiation of each donor. The maximum variation among the donors was insignificant than that

within one donor. That is, the inter-individual variation was no greater than the intra-individual variation. The intra-individual standard deviations for donors 1, 2 and 3 were 4.6%, 16.2% and 62.3%, respectively. On the other hand, the recorded inter-individual variation among the four donors 4, 5, 6 and 7 was 22.6%. One sample—from the left ring finger of donor 3—showed considerable sensitivity, as shown in Figs 3, 7, 8 and Table 1. This high sensitivity was due to a single odd data point among the 5 data points for this sample. If we remove this odd point and re-analyze the data, we obtain a sensitivity value of 0.0052. If we use this value instead of 0.013 (the sensitivity obtained by including the point that was removed), the intra-individual standard deviation of donor 3 would be 25%. This is a large deviation from 62.3%, but it did not have a significant effect on the conclusion obtained by comparing the intra-individual and inter-individual variations. The removed point was 20% larger than the estimated value when 0.0052 was used as the sensitivity. A possible reason for such a large change may be the contamination caused by small, pulverized fragments that dropped off naturally from other samples that had been irradiated with a higher dose. However, we were not able to determine the exact reason why this data point was so big.

As shown in Fig. 8, the range of the median values of the sensitivity values of fingernails from each finger position resulted in a standard deviation of only 5.4%. This is smaller than the average within each finger position, which was 25%. The fingernail position had no significant effect on sensitivity. One of the difficulties of fingernail ESR dosimetry is the large variability specific to biomaterials. Dose-response characteristics can vary depending on donors, harvest timing, sanitary conditions, etc. However, in this study, we did not find any sign of inter-individual variation in the sensitivity. One possible explanation for this unexpected result is the uncertainty in our measurements. To estimate the uncertainty, we focused on the fluctuations of the data points from the best-fit linear function shown in Fig. 2. We defined the fluctuation to be the standard deviation of the residual distribution obtained by linear regression analysis of the dose-response curves. The size of the fluctuation differed among the samples, as shown in

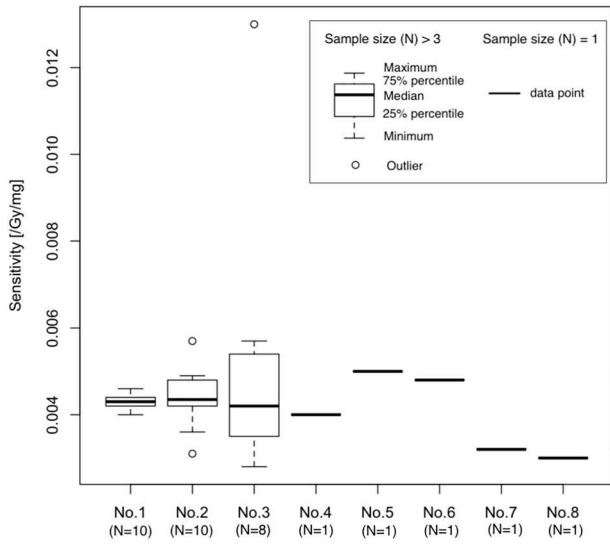


**Fig. 7.** The distribution of sensitivity for all donors in the case of the X-ray irradiation. The x-axis shows donor number. The inter-individual variation was not significantly larger than the intra-individual variation.

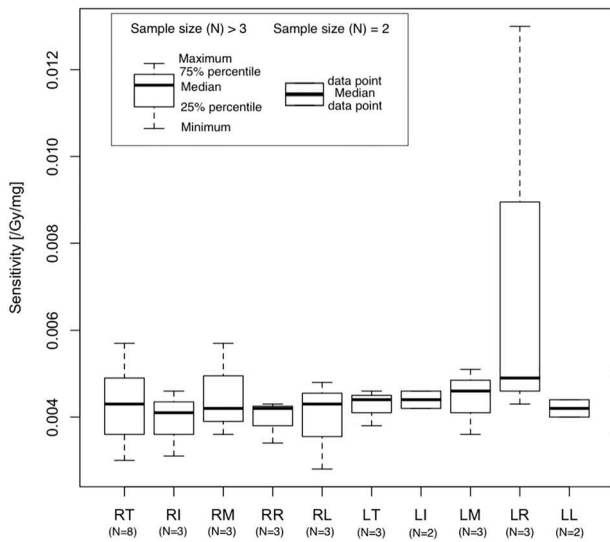


**Fig. 8.** The distribution of sensitivity for finger position in the case of the X-ray irradiation. The x-axis shows finger position of fingernail samples (RT, right thumb; RI, right index; RM, right middle; RR, right ring; RL, right baby; LT, left thumb; LI, left index; LM, left middle; LR, left ring; LL, left baby). There was no significant effect of the fingernail positions on the sensitivity.

Tables 1 and 2, but it did not depend on the sample weight or on the number of data points used to construct a dose–response curve. The average fluctuation was 1.7 Gy, with a 1.3 Gy standard deviation for X-ray irradiation. This means that there is insufficient resolution to distinguish the difference of 1.7 Gy in a single measurement with our

setup and samples. The source of this uncertainty is unclear, but this fluctuation reflects the uncertainty from all sources in our study. Based on these results, we recommend that the calibration curve should be obtained from the exposed sample for which the exposure dose is to be estimated. We cannot use unexposed samples as a sensitivity reference, even if they are from the same donor.

### DETERMINATION OF THE MIS AND BKS Determination from MIS response and direct measurement of BKS

To evaluate the MIS at harvest, the MIS response per unit cross-section of each cutting is required. The size of the MIS induced by the harvest is then given by this sensitivity multiplied by the area of the sample cross-section. A previous study showed that the size of the MIS is proportional to the number of additional cuts [11]; this means that the cutting process generates the MIS. However, these results only showed that a linear relationship exists by using the number of cuts. Thus, other researchers cannot refer to the sensitivity of MIS, because the raw values that the investigators obtained were heavily dependent on their experimental conditions. To obtain quantitative information about the MIS response, we therefore need to measure it ourselves. By making additional cuts in the samples and measuring the cross-section, we can obtain the calibration curve for the MIS and calculate the absolute response relative to the cross-section.

In addition, the MIS increment produced during transportation must be taken into consideration [2]. The rate of increase in the ambient conditions can be determined by monitoring the samples that are given additional cuts for a few days. The MIS size multiplied by this rate of increase gives the size of MIS at harvest contained in the first observed ESR signal just after the arrival of the sample.

On the other hand, it is possible to measure the BKS directly. Since the radicals decay under humid conditions, both the RIS and the MIS disappear once the samples are soaked in water [2, 10, 11]. As per the definition of the BKS, the signal that remains in the nail after eliminating both the RIS and the MIS is the BKS that is continuously generated by exposure to environmental radiation [9]. The MIS at harvest, inclusive of the increase during transportation of the unexposed sample, is then the difference between the signal prior to the irradiation and the BKS.

To confirm the validity of our method of reconstructing the MIS at harvest, we compared the estimate with a direct measurement of the BKS from samples irradiated by X-rays. We first measured the initial signal, the cross-section at harvest and the dose–response curve. Then, we erased the RIS and MIS at harvest by soaking the samples in water. We found no inconsistency in both the MIS estimation and the BKS measurement. This was our first attempt to validate this easy method to separate the RIS, MIS and BKS that does not require any complicated treatments and can be carried out in a realistic situation. The details are provided below.

### Materials and methods

#### Sample preparation and storage

From donor 4, we collected two samples for the MIS study (Table 4) and five samples for determining the BKS by eliminating the other signal components (Table 5). The storage condition was the same as



**Table 4. Sample information, thickness and sensitivity of fingernails for mechanical stimulation**

Sample information (Donor, Age, Sex)	Sample ID	Thickness [mm]	Sensitivity [1/mm <sup>2</sup> /mg]
Donor 4 (33, male)	Sample A (Right Finger, pooled)	0.55	0.010
	Sample B (Right Finger, pooled)	0.33	0.026

**Table 5. Sample information and BKS of fingernails. The details are shown in subsection 3.1.1.3**

Sample information (Donor, Age, Sex)	Sample ID	Intensity for BKS [1/mg]
Donor 4 (33, male)	Sample 1 (Right Fingers pooled)	0.077
	Sample 2 (Right Fingers pooled)	0.093
	Sample 3 (Right Fingers pooled)	0.072
	Sample 4 (Right Fingers pooled)	0.101
	Sample 5 (Right Fingers pooled)	0.110

the sensitivity study that we already discussed (Sample preparation and storage).

#### Obtaining the calibration curve and response of the MIS per unit area of cross-section

To estimate the MIS, including the signal increase during transport and storage, we measured the two right fingernail samples (samples A and B) from donor 4. Immediately after harvest, we measured the ESR signal to represent the initial state, following which we added four and three cuts to samples A and B, respectively. The details of the ESR measurements are the same as in the sensitivity study (ESR measurement). We carried out the ESR measurements after each cutting interval and we measured each cross-section of the sample with calipers. We corrected the cross-section using the ratio of arc to chord to take into consideration the curvatures of the fingernail pieces and the nail clipper. After the fourth cut to sample A, it was stored for one week to check the increase of the signal. We measured the rates of increase by monitoring sample A for 6 days.

#### Treatment to erase the RIS and MIS for BKS measurements

We used five samples from one donor and irradiated them with X-rays up to 10 Gy. After irradiation, we soaked all samples in ultrapure water for 14 hours. We then dried them for 4 days with silica gel in dark plastic bags with zipper closures. The conditions inside the bag were 20% relative humidity at 20°C room temperature. To confirm the completeness of the drying process, we measured the weight of each sample after 1.5 hours, 3 hours, 14 hours and 96 hours from when the drying commenced. We performed the ESR measurements before irradiation, soon after irradiation and after 4 days and 6 days from the start of the drying process.

## Results and discussion

### MIS estimation

Figure 9 shows the relationship between the ESR signal intensity and the total additional cross-section of the cuttings. The increment of

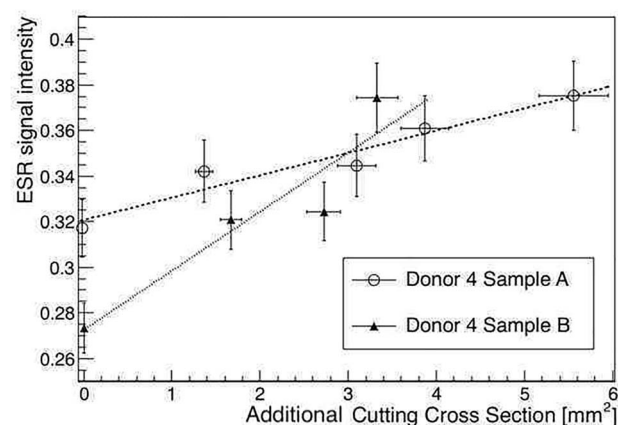


**Fig. 9. The ESR signal intensity versus total of additional cutting cross-section. The error size for cross-section was defined by propagation of the standard deviation of six measurements by the caliper. The open circle shows the result of sample A and the triangle shows the result of sample B.**

the signal intensity showed a linear response with the summation of the additional cutting cross-sections. Even in samples from the same donor, the response to cutting varied across samples. The responses of samples A and B were  $(0.010 \pm 0.003)/\text{mm}^2$  and  $(0.026 \pm 0.005)/\text{mm}^2$ , respectively. The typical fingernail thickness was around 0.5 mm and the width was about 1 cm. A rough estimate of the size of the MIS generated at harvest is comparable to the size of the RIS generated by 20 Gy X-ray irradiation if we assume the average of the MIS response and the typical sensitivity for X-ray irradiation shown above.

From a follow-up study of sample A, the MIS signal intensity increased by 5.5% after 12 hours, 12% after 4 days and 16% after 6 days. This trend is consistent with Romanyukha *et al.* [15]. Based on Fig. 4 in Romanyukha *et al.* [15], the MIS will continue to increase up to about 130% in excess of the initial state. If we measure the MIS sensitivity, the cross-section at the harvest, the rate of increase and the elapsed time from harvest to the measurement for each sample, we can

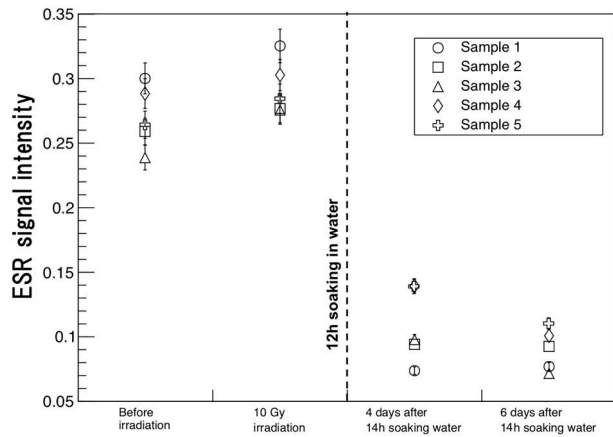


**Fig. 10.** The ESR signal intensity across four stages in our signal elimination experiment. We tried to eliminate both the RIS and MIS by soaking samples in water between stages 2 and 3. Stage 1—before irradiation; stage 2—just after 10 Gy X-ray irradiation; stage 3—after 4 days of drying; stage 4—after 6 days of drying. The signal sizes in stages 3 and 4 were expected to be the size of BKS.

estimate the contribution of the MIS to the ESR signal retrospectively. We recommend that all these characteristics be measured from the accident-exposed sample. However, the MIS at harvest is expected to be large compared to the RIS, so a significant reduction in uncertainty will be necessary in order to obtain the RIS generated by a few Gy of X-rays.

#### BKS estimation

To estimate the initial state of the fingernail signal before irradiation from an accident, we erased all the signals, including the RIS, by soaking the additional five samples (see Table 5) in water [10, 16]. These samples were irradiated with 10 Gy of X-rays before this treatment. The samples absorbed water during 14 hours of soaking and this increased their weight by  $29 \pm 8\%$  on average. The error is the standard deviation of all the samples. After 14 hours of storage alongside silica gels, the samples were almost dry. After 4 days, they were ready. The remaining increment of weight after 14 hours was  $2.5 \pm 1.9\%$ , and that after 4 days it was  $-1.2 \pm 2.1\%$ . Figure 10 shows the ESR signal intensity of the five samples at each stage of this procedure. First, we measured the initial state of ESR signals that are expected to include the MIS at harvest. Second, we measured the ESR signal immediately after 10 Gy irradiation with X-rays. These signals should contain the RIS, MIS and BKS. Then, we erased the RIS and MIS by soaking the samples in water for 14 hours. We carried out the third measurement 4 days after this step. Finally, we measured the samples again 2 days later to check the time-dependence of the BKS. There was no signal increase. In fact, the signal decreased between the third and fourth measurements, which is consistent with the definition of BKS in Bonazzola *et al.* [8]. Therefore, we conclude that the signal we measured is in fact the BKS. For the 10 Gy X-ray exposure, 14 hours was enough time to erase all the signals. Further study is needed to determine how much soaking time is needed for a higher exposed dose.

In our study, the sizes of the BKS were varied in different samples from the same donor. The average of the BKS was 0.090, and it was the same size as the RIS obtained with 21 Gy of X-rays if we use the average sensitivity, 0.0043/Gy/mg. The standard deviation of the BKS corresponded to 3.3 Gy. This is larger than the measured uncertainty due to the vertical sample position for this signal size. The BKS should also be measured from the exposed sample in the actual case.

The difference between the ‘before irradiation’ and ‘after 12 hours of soaking in water’ signal intensity values in Fig. 10 are thought to be the values of the MISs at harvest. These estimates of the MIS are the same size as the RIS—about 42 Gy. These samples were stored for almost 8 months after harvest. Based on Fig. 4 in Romanyukha *et al.* [15], the MIS increase was saturated after about 50 days, at which time the signal size reached 2.3 times that of the initial MIS. Applying this result to our study, we find that the initial size of the MIS should be about 18 Gy, based on the RIS ( $42 \text{ Gy}/2.3 \sim 18 \text{ Gy}$ ). This value is consistent with the expected size of the MIS at harvest, around 20 Gy.

These results show no inconsistency between the MIS and BKS estimate. Thus, this easy method to remove the MIS and BKS from the measured ESR signal of exposed samples can be used in an actual case without having to perform complicated treatments on the samples.

#### Determination from non-irradiated samples after cutting

Another way to separate the MIS and BKS from the RIS is to determine the typical signal size for non-irradiated samples. The observed signal from a non-irradiated sample just after harvest should be the convolution of the MIS and BKS. In principle, all samples should contain both the MIS at harvest and the BKS. If we can determine the sum of the MIS and BKS from the measurements of non-irradiated samples, and if we find the distribution of non-irradiated samples to be small enough, we can estimate the RIS quicker than through the method described above. To reduce the inter-individual variation, we also tested the use of the toenail samples as a control. In the expected case of radiation accidents in the medical environment, only the hand may be exposed because feet are likely to have been inside the safety shoes. Thus, if toenail samples have similar characteristics to fingernails, they can be used as control samples.

To verify whether this method can be of service, we measured non-irradiated samples and toenails.

#### Materials and methods

We collected 144 samples from eight donors to determine the distribution of non-irradiated samples (see Table 6). From donor 2, we also collected toenails to compare them with fingernails (Table 7). The ESR measurement conditions were the same as in section 2.

#### Results and discussion

Figure 11 shows the distribution of the ESR signals from non-irradiated fingernails. The average of the signal was 0.25, the mode

**Table 6. Donor information for the measurement of non-irradiated fingernail samples.** ‘Collection frequency’ indicate how many times donors provided samples. If this number is ‘1,’ they provided all fingernail samples at one time. We divided all samples into 144 samples

Donor information (Donor, Age, Sex)	Collection Times for non-irradiated signals
Donor 3 (34, male)	4
Donor 4 (33, male)	4
Donor 6 (34, female)	3
Donor 8 (62, female)	1
Donor 9 (39, female)	1
Donor 10 (45, male)	1
Donor 11 (65, male)	1
Donor 12 (31, male)	1

**Table 7. Sample information and sensitivity of toenails in the X-ray irradiation case**

Sample information (Donor, Age, Sex)	Toenail position	Sensitivity [ /Gy/mg]
Donor 2 (49, male)	Right Thumb	0.002350
	Right Index	0.003047
	Right Middle	0.004428
	Right Ring	0.001827
	Right Little	0.002823
	Left Thumb	0.003031
	Left Index	0.003724
	Left Middle	0.003241
	Left Ring	0.003631
	Left Little	0.003876

was 0.11 and the standard deviation was 0.139. These values corresponded to 53 Gy, 25 Gy and 30 Gy, respectively, assuming the typical sensitivity for X-rays. According to our rough estimate of the MIS at harvest (~20 Gy), its increase (1 ~ 2.3 times), the BKS (~20 Gy), and the sensitivity (0.0043/Gy/mg), the distribution should range between 0.17 to 0.28. However, the distribution was actually more extended than this. To understand this extension, we need to collect more data about the MIS and BKS to determine the variation of sensitivity due to mechanical stimulation and the intensity of the BKS.

We also determined the distribution of the ESR signal from non-irradiated toenails, as shown in Fig. 12. The average was 0.11 and the standard deviation was 0.014. This distribution tended to be lower than for the fingernails, but it was still within the range of the fingernail distribution. Much more data is needed to decide whether toenails can be used to estimate the zero point for the calibration curves.

We also checked the sensitivity of toenails to X-ray irradiation. Figure 13 and Table 7 show the distribution of the sensitivity of toenails and fingernails from this one donor. There was a tendency for the sensitivities of the toenails to be smaller than those of the fingernails.

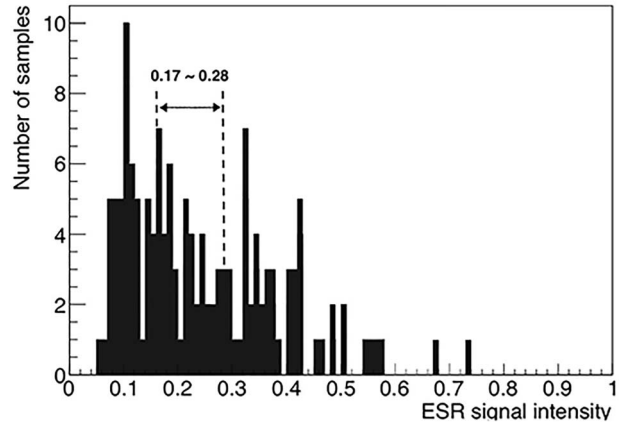


**Fig. 11. The distribution of ESR signals of 144 non-irradiated fingernail samples from eight donors.** The ESR signals should contain BKS and MIS generated at harvest. The MIS was increased for the storage time. The range we noted (0.17 ~ 0.28) in this histogram shows the rough estimation of the width of signal size when we take BKS, MIS and its increase under storage conditions into consideration.

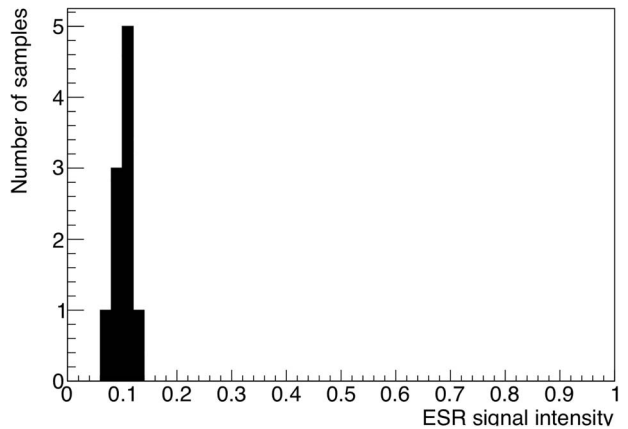


**Fig. 12. The distribution of ESR signals of non-irradiated toenails from donor 2.** The average was 0.11 and the standard deviation was 0.014. This distribution tended to be lower than that of fingernails, but it was still within the range of the fingernail distribution.

The Wilcoxon rank-sum test rejected the hypothesis that the mother distribution of the toenail sensitivity was the same as that of fingernails, with a p-value of 0.00039. This result supports our recommendation to obtain the calibration curve from the exposed samples themselves.

These results show that we cannot estimate the MIS at harvest from non-irradiated control samples in order to reconstruct the RIS due to an accident. We recommend that all properties—X-ray sensitivity, MIS sensitivity, MIS rate of increase and BKS—be measured from the same exposed sample in order to evaluate the RIS produced by accidental exposure.

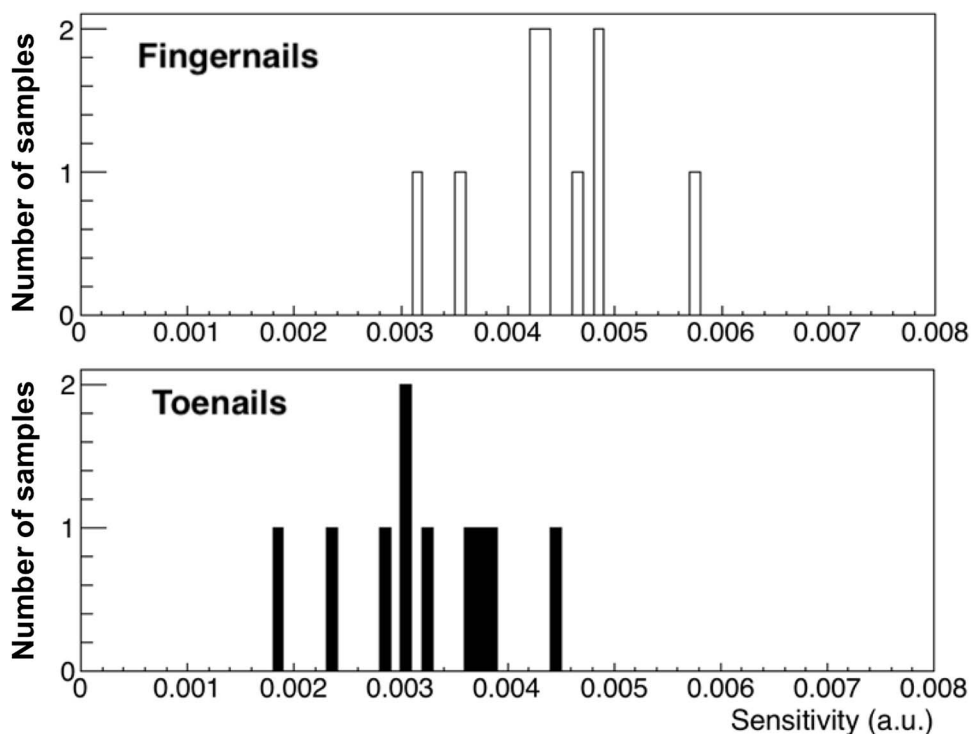


Fig. 13. The distribution of fingernail and toenail sensitivity for X-rays from donor 2. The top histogram is for fingernails and the bottom is for toenails. The sensitivity of toenails was lower than that of fingernails.

#### PROPOSAL OF NEW PROCEDURE FOR NAIL ESR DOSIMETRY

Based on the results obtained in this work, we propose the following procedure for X-band fingernail ESR:

1. Store the fingernail samples with silica gel in a plastic bag and send it to a laboratory.
2. Measure the weight and cutting cross-section of each sample piece.
3. Measure the ESR signal before any treatment.
4. Obtain the calibration curve by using radiation with a sensitivity that is similar to the one in question.
5. Erase all signals by soaking the samples in water and drying them completely.
6. Measure the BKS.
7. Add new cuts and calculate the sensitivity to cutting.
8. Determine the increase of the MIS under ambient conditions for the same period as from harvest to the first measurement.
9. To determine other factors, erase all signals and measure the effect of those specific factors.

This proposed protocol is different from a previous recommendation [5] in terms of the handling of the MIS. In Tromprier *et al.* [5], the authors proposed eliminating the MIS generated on the surface of the cut edges of samples soon after cutting by applying a wet brush (this protocol has not been finalized). In contrast, our protocol mandates the measurement of the MIS sensitivity for each sample and the estimation of the MIS generated at harvest. We propose evaluating the MIS because the process required to eliminate it may be too complicated for use by the people on-site, such as the subject or clinical staff, who will harvest the subject's nails. Also, it avoids the additional uncertainties due to variations in the degree of elimination.

The conditions for a long period of storage in the laboratory can be selected based on previous studies if an MIS increase is to be avoided. From our experience, freezing a sample at  $-20^{\circ}\text{C}$  stopped this increase. However, a great amount of uncertainty still remains, and further studies to reduce it are necessary before using the proposed fingernail dosimetry in actual accidents in a medical environment.

#### CONCLUSION

In this study, we investigated the dosimetric properties of the ESR signals from fingernails irradiated by X-rays. These properties are essential for reconstructing the exposed dose retrospectively.

According to the dose–response curves, the size of the RIS is proportional to the X-ray dose, as in the case of  $\gamma$ -ray irradiation. Fingernails are equally sensitive to X-rays and  $\gamma$ -rays of the same air-absorbed dose. The effect of secondary electrons on the net absorbed dose of fingernails did not make a significant difference in the case of both X-rays and  $\gamma$ -rays. The sensitivity did not depend on the individual or on the finger position. The intra-individual variation was commensurate to the inter-individual variation.

To determine the zero point of the calibration curve, we needed to estimate both the MIS and BKS or their convolution. We also checked the relationship between the MIS and cross-sections of the nail cutting. The MIS seems to be proportional to these cross-sections. The MIS sensitivity differed across samples, even when the samples came from one donor. Also, we observed an increase in the MIS with time, as previously reported. If a very rough estimate of a cutting cross-section at harvest is  $0.5\text{ mm}^2$ , then the typical intensity of the MIS at harvest

would be about 20 Gy—comparable to the RIS produced by X-rays if we use the average sensitivity value we obtained in this study. We showed that the BKS can be measured after eliminating both the RIS from 10 Gy of X-rays and the MIS at harvest by soaking the samples in water for 14 hours. The size of the BKS corresponded to 20 Gy, which is comparable to the RIS produced by X-rays if we calculate it in the same way as for the MIS at harvest.

We also determined the distribution of 144 non-irradiated fingernail samples from eight donors and we obtained data from 10 toenail samples before irradiation. The former had a wider distribution than expected based on our rough estimates of the MIS and BKS. More measurements of the MIS and BKS are required to determine the variation of the MIS and BKS, which may explain the greater width of this non-irradiated fingernail distribution. The latter showed no significant difference from the fingernail distribution, unlike in the case of the sensitivity to X-rays.

Based on these results, we recommend that the dosimetric properties (sensitivity of the RIS and MIS and the intensity of the BKS) should be measured using exposed samples. Using typical values for these properties from many samples or from standard samples in dose reconstruction would increase the error size due to the inter-sample variation among these values.

Based on the results obtained in this work, we proposed a new procedure for X-band fingernail ESR in section 4.

#### ACKNOWLEDGEMENTS

This study was partially supported by MEXT/JSPS KAKENHI Grant Number 18KK0147 and the Program of the Network-type Joint Usage/Research Center for Radiation Disaster Medical Science.

#### REFERENCES

- Dalgarnov B, McClymont J. Evaluation of ESR as a radiation accident dosimetry technique. *International Journal of Radiation Applications and Instrumentation Part A Applied Radiation and Isotopes* 1989;40:1013–20.
- Reyes R, Tromprier F, Romanyukha A. Study of the stability of EPR signals after irradiation of fingernail samples. *Health Phys* 2012;103:175–80.
- Wang L, Wang X, Zhang W et al. Determining dosimetric properties and lowest detectable dose of fingernail clippings from their electron paramagnetic resonance signal. *Health Phys* 2015;109:10–4.
- Tipikin D, Swarts S, Sidabras J et al. Possible nature of the radiation-induced signal in nails: high-field EPR, confirming chemical synthesis, and quantum chemical calculations. *Radiat Prot Dosimetry* 2016;172:112–20.
- Tromprier F, Kornak L, Calas C et al. Protocol for emergency EPR dosimetry in fingernails. *Radiat Meas* 2007;42:1085–8.
- Tromprier F, Queinnec F, Bey E et al. Bottollier-Depois, Epr retrospective dosimetry with fingernails: Report on first application cases. *Health Phys* 2014;106:798–805.
- Chandra H, Symons M. Sulphur radicals formed by cutting alpha-keratin. *Nature* 1987;328:833–834.
- Bonazzola L, Fackir L, Leray N et al. ESR study of some sulfur-centered radicals formed in irradiated cysteamine and 1,4-dithiane single crystals. *Radiat Res* 1984;97:462–7.
- Symons M, Chandra H, Wyatt J. Electron paramagnetic resonance spectra of irradiated finger-nails: a possible measure of accidental exposure. *Radiat Prot Dosimetry* 1995;58:11–5.
- Reyes R, Romanyukha A, Tromprier F et al. Electron paramagnetic resonance in human fingernails: the sponge model implication. *Radiat Environ Biophys* 2008;47:515.
- Tromprier F, Romanyukha A, Reyes R et al. State of the art in nail dosimetry: free radicals identification and reaction mechanisms. *Radiat Environ Biophys* 2014;53:291–303.
- Black P, Swarts S. Ex vivo analysis of irradiated finger nails: chemical yields and properties of radiation-induced and mechanically-induced radicals. *Health Phys* 2010;98:301.
- Strzelczak G, Sterniczuk M, Sadlo J et al. EPR study of gamma-irradiated feather keratin and human fingernails concerning retrospective dose assessment. *Nukleonika* 58.
- Symons M. Formation of radicals by mechanical processes. *Free Radic Res Commun* 1988;5:131–139.
- Romanyukha A, Tromprier F, LeBlanc B et al. EPR dosimetry in chemically treated fingernails. *Radiat Meas* 2007;42:1110–3.
- Marciniak A, Ciesielski B, Prawdzik-Dampc A. The effect of dose and water treatment on EPR signals in irradiated fingernails. *Radiat Prot Dosimetry* 2014;162:6–9.
- Chiyoda TECHNOL. *DoseAce/FGD-1000*. <http://isotope.c-technol.co.jp/pdf/DoseAce1407ATG.pdf>
- Sato T, Iwamoto Y, Hashimoto S et al. Features of particle and heavy ion transport code system (phits) version 3.02. *Jour Nucl Sci Tech* 2018;55:684–90.
- Baswan S, Kasting G, Li S et al. Understanding the formidable nail barrier: a review of the nail microstructure, composition and diseases. *Mycoses* 2017;60:284–95.